Lineshape of rotational spectrum of CO in ⁴He droplets

Robert E. Zillich,[1,2,a)] K. Birgitta Whaley,[3,4] and Klaus von Haeften[5]

[1]*Fraunhofer ITWM, 67663 Kaiserslautern, Germany*
[2]*Institut für Theoretische Physik, Johannes Kepler Universität, A-4040 Linz, Austria*
[3]*Department of Chemistry, University of California, Berkeley, California 94720, USA*
[4]*Pitzer Center for Theoretical Chemistry, University of California, Berkeley, California 94720, USA*
[5]*Department of Physics and Astronomy, University of Leicester, Leicester LE1 7RH, United Kingdom*

In a recent experiment the rovibrational spectrum of CO isotopomers in superfluid helium-4 droplets was measured, and a Lorentzian lineshape with a large line width of 0.024 K (half width at half maximum) was observed [von Haeften *et al.*, Phys. Rev. B **73**, 054502 (2006)]. In the accompanying theoretical analysis it was concluded that the broadening mechanism may be homogeneous and due to coupling to collective droplet excitations (phonons). Here we generalize the lineshape analysis to account for the statistical distribution of droplet sizes present in nozzle expansion experiments. These calculations suggest an alternative explanation for the spectral broadening, namely, that the coupling to phonons can give rise to an inhomogeneous broadening as a result of averaging isolated rotation-phonon resonances over a broad cluster size distribution. This is seen to result in Lorentzian lineshapes, with a width and peak position that depend weakly on the size distribution, showing oscillatory behavior for the narrower size distributions. These oscillations decrease with droplet size and for large enough droplets ($\sim 10^4$) the line widths saturate at a value equal to the homogeneous line width calculated for the bulk limit. © *2008 American Institute of Physics*. [DOI: 10.1063/1.2833979]

I. INTRODUCTION

The reduction of the rotational excitation energies of molecules in superfluid helium-4 has been observed in many experiments (see table in Ref. 1) and has been studied extensively by quantum Monte Carlo simulations,[2–5] by phenomenological approaches based on the two-fluid picture[6,7] or hydrodynamics of ideal fluids,[8] and by quantum many-body theory.[9,10] In principle, this is now a well-understood phenomenon: The molecule aquires an increased effective moment of inertia by coupling to excitations of the ⁴He environment that may be local or collective, depending on the nature of the molecule and its interaction with helium. There is considerable less understanding of the *shape* of the spectrum, namely, whether the transitions are broadened homogeneously or inhomogeneously, and what the broadening mechanisms are. The spectral lineshapes for rovibrational transitions of some species are markedly non-Lorentzian[11–13] and in some cases also show a dependence on the *J* quantum number.[11] Other species show Lorentzian lines[14–19] but whether this is due to rotational or vibrational relaxation or has an inhomogeneous origin is generally not clear. We note that inhomogeneous broadening is usually associated with non-Lorentzian line profiles. However, there do exist situations in which inhomogeneous broadening can yield Lorentzian lineshapes, for example, in the spectra of color centers in crystals with point defects[20] (e.g., optical spectra of impurities[21]) and dipole coupled spins in solids.[22]

It has been speculated that Lorentzian line profiles for small molecules with large rotational constants are due to rotational relaxation proceeding via coupling to bulk modes of the droplet.[23] A microscopic theory for such coupling was advanced in Ref. 24 and applied to evaluation of linewidths for CO.[15] This approach will be discussed and refined for finite droplet sizes below. Earlier theoretical works focused on analyzing the effects of confinement in the cluster, which introduces inhomogeneous broadening, and the contribution of hydrodynamic backflow and excitation of surface modes (ripplons) to inhomogeneous broadening.[25] Since hydrodynamic modes result from long wavelength phonon modes,[24] this represented a first attempt at understanding the role of coupling to helium excitations in the line widths. It was estimated that the role of ripplon excitations is negligible compared to the effect of anisotropy in the confinement potential. Applications were made to HCN and to OCS. For the heavier molecule, OCS, numerical estimates for the *R*(0) line were in fair agreement with existing experimental data,[26] but the theory could not account for *J* dependent asymmetry and spectral tails. Subsequent experiments for HCN and DCN showed narrower lines [a factor of 6 narrower than the theoretical prediction for HCN, although the shape of the line (not shown) was stated to be in good agreement with the predictions of Ref. 25].

In this paper we focus on the lineshape of a light molecule CO. The rovibrational depletion spectrum of CO in large ⁴He droplets was recorded in Ref. 15 and the *R*(0) line found there to be of Lorentzian shape. As outlined in Refs. 10 and 24, correlated basis function (CBF) theory coupled with diffusion Monte Carlo (DMC) simulations for ground state properties yields an homogeneous Lorentzian lineshape

a)Electronic mail: robert.zillich@jku.at.

for the rotational spectrum in the limit of infinite droplet size (bulk limit), which is due to direct coupling of the rotational excitations to the two continua provided by bulk phonons of the helium and by translational momentum (recoil) of the molecule, respectively. Explicit calculations made for CO in Ref. 15 resulted in a prediction of a Lorentzian line with a width of 0.013 K [half width at half maximum (HWHM)], confirming that rotational relaxation can provide the correct lineshape but with a line width smaller than the corresponding experimental value of 0.024 K that was measured in helium droplets. Given the numerical uncertainties of the ^{4}He distribution around CO obtained by DMC simulations (which enters quadratically into the CBF calculation of the spectrum) and the neglect of possible surface excitations (ripplons) and of thermal broadening, this calculated line width value was deemed to be in fair agreement with the experimental droplet value. A point of contention here is the fact that the phonon density of states for droplets in the size regime typically achieved in the experiment (on the order of a few thousand He atoms) is much too low to allow homogeneous broadening. In Ref. 15 it was estimated that the high density of states necessary for homogeneous broadening could be provided by the particle-in-a-box states of the molecule solvated in the He droplet. It was consequently concluded in Ref. 15 that the mechanism responsible for line broadening is the relaxation of the rotational excitation by coupling to collective excitations (phonons) of the ^{4}He droplet, and that the lineshape is thus likely indeed due to homogeneous broadening.

In this work we present CBF calculations which suggest an alternative explanation of the measured Lorentzian lineshape for the $R(0)$ rotational transition state of CO in ^{4}He droplets coupled to the discrete phonon spectrum, namely, an inhomogeneous Lorentzian broadening of rotation/phonon resonances that results from the droplet size distribution in the experimental preparation of the He droplets.[27] Here, the physical process underlying this inhomogeneous broadening is resonant phonon-rotation coupling, i.e., the finite size analog of the process causing homogeneous broadening in the bulk limit, namely, relaxation of the rotational excitation by phonon excitation. In the following section we derive an approximate model for finite sized droplets that is based on a modification of the CBF approach for molecules in bulk helium. Using this model, we are able to average the explicitly calculated size-dependent absorption spectra over the droplet size distribution. In Sec. III we then present calculations made assuming the log-normal distribution established for helium droplets.[27] These calculations show that the resulting inhomogeneous spectrum for the $R(0)$ rotational absorption of CO has a Lorentzian lineshape just like the homogeneous bulk spectrum. Both the width and peak position of the spectral line show variations with $\bar{N}$ that are oscillatory for a range of droplet size distributions. These oscillations decrease with average cluster size and the saturation values of both linewidth and peak position for droplets larger than $\bar{N} \sim 10^4$ become approximately independent of the size distribution. In particular, the line width is then essentially the same as that in the bulk, although it is still broadened inho-

mogeneously at these finite $\bar{N}$. A detailed comparison of our droplet lineshape calculations with the experimental measurements that were reported in Ref. 15 for average droplet sizes varying from $\bar{N} \sim 1200$ to $\bar{N} \sim 3600$ shows very good qualitative agreement with the size dependence of both line width and peak position. This analysis of the size dependence of the spectral lineshapes shows that, in principle, this theory would allow details of the droplet size distributions to be extracted from experimentally measured lineshapes for a broad range of droplet sizes. Our analysis also suggests that it would be extremely valuable to analyze the lineshapes in droplets smaller than $\bar{N}=1000$ with a detailed comparison between theory and experiment. However, given the inefficiency of measuring infrared absorption by depletion for CO, it remains an experimental challenge to close the gap between $\bar{N} \sim 100$ and $\bar{N} \sim 1000$ atoms.[28,29]

Recently, a simple analytic model has been introduced for the absorption lineshape of a single bright state (e.g., a rotational excitation) interacting with a set of equally spaced bath levels (e.g., discrete phonons), given a mechanism for inhomogeneously shifting the position of the bath levels relative to the bright state.[30] Assuming that the inhomogeneity mechanism results from some size dependence of the bath levels, such as seen in the phonon levels of a finite cluster, this analytic model predicts an inhomogeneous but Lorentzian broadening of the absorption spectrum of the bright state, consistent with our CBF results for CO in ^{4}He droplets. In addition to accounting for the inhomogenous Lorentzian lineshapes, the CBF theory also accounts for the size dependence of the lineshape features and provides a microscopic description of the coupling of the molecule to the bath levels.

II. MODIFIED CBF THEORY FOR ROTATIONAL EXCITATIONS IN FINITE DROPLETS

We present a model for rotational excitations of a molecule in a finite ^{4}He droplet that is based on our previous CBF theory for molecules in bulk ^{4}He in Ref. 24. The rotational self-energy for a linear molecule of mass M_0 and rotational constant B_0 in bulk ^{4}He is given by the following expression:

$$\Sigma_b(\omega) = -B_0^2 \frac{(4\pi)^2 \rho}{2J+1} \sum_\ell \int \frac{dp\,p^2}{(2\pi)^3} \frac{1}{S(p)}$$
$$\times \frac{\sum_{\ell'} \tilde{L}(J,\ell',\ell) g_{\ell'}^2(p)}{B_0 \ell(\ell+1) + \epsilon(p) + \hbar^2 p^2/2M_0 - \hbar\omega}, \quad (1)$$

where the subscript b denotes bulk. Here $\epsilon(p)$ is the phonon-roton dispersion of bulk ^{4}He and $S(p)$ is the static structure factor. Both are taken from experimental measurements. ρ is the bulk density and $g_{\ell'}(p)$ is the Legrendre-Bessel transform of the CO–He pair distribution function which we obtained by DMC simulation.[15] $g_{\ell'}(p)$ and $\tilde{L}(J,\ell',\ell)$ are defined in Ref. 24. $\tilde{L}(J,\ell',\ell)$ is proportional to the square of the 3-j symbol

$$\begin{pmatrix} J & \ell' & \ell \\ 0 & 0 & 0 \end{pmatrix}$$

and thus provides selection rules. In bulk helium the phonons of wave vector p are plane waves $e^{i\mathbf{p}\mathbf{r}}$ which come from the Feynman ansatz for the N-body wave function $\Psi(\mathbf{r}_1, \ldots, \mathbf{r}_N) = \sum_j e^{i\mathbf{p}\mathbf{r}_j} \Psi_0(\mathbf{r}_1, \ldots, \mathbf{r}_N)$, where Ψ_0 is the ground state wave function. Equivalently, we can use spherical Bessel functions $j_{\ell'}(pr)$ and spherical harmonics $Y_{\ell'm}(\Omega)$ instead of plane waves, since for given p, and hence for given $\epsilon(p)$, these bases can be interconverted, $e^{i\mathbf{p}\mathbf{r}} = 4\pi\sum_{\ell',m} i^{\ell'} j_{\ell'}(pr) Y^*_{\ell'm}(\Omega_k) Y_{\ell'm}(\Omega_r)$. This allows us to interpret the expression (1) for $\Sigma_b(\omega)$: The rotational excitation J couples to rotational excitations ℓ and phonon modes of angular momentum ℓ' and momentum p, causing an effective moment of inertia that is larger than the momentum of inertia of the bare molecule. If the coupling is such that energy is conserved [the denominator in Eq. (1) vanishes], the rotational excitation J can decay by exciting a rotational excitation $\ell < J$ and a phonon. For $J=1$ [the $R(0)$ transition], this means that $\ell = 0$ (decay into rotational ground state) and therefore, as a result of the selection rules incorporated in $\tilde{L}(J, \ell', \ell)$, the only phonon modes that can be excited are $\ell' = 1$ modes.

Using Eq. (1), the pure rotational (microwave) absorption spectrum is then obtained by standard methods of the linear response theory,[10]

$$S_b(\omega) = \frac{1}{\pi} \operatorname{Im}[\hbar\omega - B_0 J(J+1) - \Sigma_b(\omega)]^{-1}$$

$$= \frac{\operatorname{Im}\Sigma_b(\omega)/\pi}{(\gamma_J(\omega) - \hbar\omega)^2 + (\operatorname{Im}\Sigma_b(\omega))^2}, \quad (2)$$

where we have defined $\gamma(\omega) = B_0 J(J+1) + \operatorname{Re}\Sigma_b(\omega)$. $\operatorname{Im}\Sigma_b(\omega)$ is the rotational line width in bulk ^{4}He, and $\operatorname{Re}\Sigma_b(\omega)$ determines the shift of the spectral line and hence the effective molecular rotational constant in helium.[15]

This theory was developed for the rotational excitation of a linear molecule in bulk helium at zero temperature and assuming no initial molecule momentum. Both phonon/roton modes and the recoil energies in the denominator of Eq. (1) are continuous and Eq. (1) implicitly contains a double continuum which due to momentum conservation collapses to a single p-integration (see Ref. 24). We now extend Eq. (1) to finite helium droplets of radius R. We shall do this by changing one of these two continua, namely, the phonon/roton spectrum, to a discrete spectrum. As described below, treating the translational motion of the molecule classically allows the second continuum to be retained in a first approximation, and also retains the rotational symmetry of the original bulk problem, thus breaking only translational symmetry. The full quantum treatment of the translational molecule motion will be addressed in a more complete analysis elsewhere. We shall restrict ourselves here to analysis of the effect of the droplet size on the phonon-molecule coupling.

Our finite cluster model is characterized by the following assumptions:

(1) The phonon spectrum in a droplet is discrete, which we achieve by assuming that the radial part of the phonon wave function vanishes at the droplet surface, $j_\ell(pr) = 0$ for $r = R$. This leads to discrete phonon wave numbers $p_\ell^{(i)}$.

(2) The translational motion of the molecule will be treated classically so that at $T = 0$ the molecule will be initially located in the center of the droplet as a result of the confinement potential. The translational energy will be continuous, i.e., any recoil energy is allowed. Hence we neglect the discrete nature of the molecule translational motion in the droplet as well as the contribution of thermal effects.

(3) We neglect surface excitations (referred to as "ripplons" in case of the free surface for helium[31]). When the molecule is initially located at the center of the droplet this will be rigorously true because only collective modes with $\ell' = 1$ can be excited by the molecule rotation excitation $J = 1$, while the lowest ripplon mode has $\ell' = 2$.

Since there is no coupling to ripplons in this model when the molecule is located at the cluster center, the main difference from the previous theory employing bulk excitations is then the discretization of the cluster phonon/roton modes. A more complete analysis would allow the molecule to move not just classically with continuous energy, but with quantized translational levels in the effective confinement potential provided by the cluster, as in Ref. 25. Quantized translation also introduces, in principle, the possibility of the nonzero coupling of the molecule to ripplons but this was found to be negligible in Ref. 25. Note that while Ref. 25 made a more realistic analysis of the molecular translational motion than is given here, it utilized only a simple phenomenological model of the molecular rotation and helium coupling, namely, that of a rotating ellipsoid coupled to hydrodynamic modes. In contrast, the present theory contains a microscopic description of the coupling between molecular rotation and helium.

With this discrete phonon model the rotational self-energy of a molecule in a finite ^{4}He droplet of radius R becomes

$$\Sigma_R(\omega) = -B_0^2 \frac{\rho}{2J+1} \sum_\ell \sum_i \frac{1}{S(p_\ell^{(i)})}$$

$$\times \frac{\sum_{\ell'} \tilde{L}(J, \ell', \ell)(g_{\ell'}^{(i)})^2}{B_0 \ell(\ell+1) + \epsilon(p_{\ell'}^{(i)}) + \hbar^2 (p_{\ell'}^{(i)})^2 / 2M_0 - \hbar\omega}, \quad (3)$$

where the subscript R now denotes the dependence on radius. Here $p_\ell^{(i)}$ is obtained by solving

$$j_\ell(p_\ell^{(i)} R) = 0,$$

and $g_\ell^{(i)}$ is the expansion of the pair distribution $g(r, \cos\theta)$ in the discrete phonon basis,

$$g_\ell^{(i)} = \frac{1}{\mathcal{N}} 2\pi \int d\cos\theta \int dr r^2 P_\ell(\cos\theta) j_\ell(p_\ell^{(i)} r)$$

$$\times [g(r, \cos\theta) - 1],$$

with the normalization $\mathcal{N}^2 = \int dr r^2 j_\ell(p_\ell^{(i)} r)^2$. We see from the denominator of Eq. (3) that the molecule now couples to discrete phonon modes. Figure 1 shows the discrete phonon excitations for a cluster of size $N = 3000$. We note that while most of these excitations are higher in energy than the molecular $J=1$ rotational energy, they nevertheless have finite coupling amplitudes and, when summed over all ℓ' values, produce a sizeable self-energy $S_R(\omega)$ that causes a reduction in the effective rotational constant. Next we discuss $S_R(\omega)$ as function of cluster radius R.

First, we point out that formally, only after taking the bulk limit, $\lim_{R\to\infty} \Sigma_R(\omega) = \Sigma_b(\omega)$, whereupon the discrete sum Σ_i becomes an integral over continuous wave numbers p does the self-energy gain an imaginary contribution $\mathrm{Im}\,\Sigma_b(\omega)$. Regardless of how large the droplet radius R is, as long as $R < \infty$ the self-energy $\Sigma_R(\omega)$ is real. For any finite R, the spectrum $S_R(\omega)$ of a molecule in a helium droplet consists then of a number of δ functions,

$$S_R(\omega) = \frac{1}{\pi}\,\mathrm{Im}[\hbar\omega - B_0 J(J+1) - \Sigma_R(\omega) - i\epsilon]^{-1} \quad (4a)$$

$$= \sum_i^M a_i \delta(\hbar\omega - \hbar\omega_i). \quad (4b)$$

Here ω_i are the zeros of

$$\hbar\omega = B_0 J(J+1) - \Sigma_R(\omega), \quad (5)$$

and the spectral weights are given by

$$a_i = \left(1 - \frac{\partial \Sigma_R}{\partial \hbar\omega}\right)^{-1}_{\omega=\omega_i}, \quad (6)$$

where we have expanded the energy denominator in Eq. (4a) about the zeros ω_i and have also used $1/(x-x_0-i\epsilon) = P(1/(x-x_0)) + i\pi\delta(x-x_0)$. However, for very large but still finite R, there will be many nonzero spectral weights a_i and the envelope of the corresponding lines will be of Lorentzian shape.[32] Since the spectral resolution is limited in experiments and the lines are broadened by the finite resolution of the spectrometer, the overall spectrum will then resemble a continuous Lorentzian spectrum as in Eq. (2). Thus, for very large R, the underlying physics is that of homogeneous broadening, in that the rotational excitations interact with a very densely spaced set of phonon levels that act as a quasicontinuum.

In order to reach this homogeneous broadening or quasicontinuum limit, the states that the molecule rotational degrees of freedom couple to must be dense compared to the line width. In the present case, molecular rotation states can couple to phonons of the droplet. For a typical helium droplet size of a few thousand atoms, only one or two weights a_i are non-negligible and all other weights are insignificantly small, as we shall see below. This is the result of the large spacing of the phonon levels noted above. For low energy

phonons this is of the order of 1 K (see Fig. 1), i.e., almost two orders of magnitude larger than the experimentally observed line width of 0.024 K/0.017 cm^{-1} (HWHM) for the $R(0)$ line of CO in helium droplets.[15,42] Other modes that might couple to the molecular rotation are the surface ripplon modes and the molecular translational motion, as discussed in, e.g., Ref. 25. Ripplons have a higher density of states, but this is still far too low to account for the measured broadening. In Ref. 15 it was estimated that taking into account the density of particle-in-a-box states of the CO molecule could yield a sufficiently high density of phonon$\times$particle-in-a-box product states to yield a homogeneous lineshape.

In the next section, we demonstrate that the simple CBF model for rotational excitations in finite droplets described above leads to an alternative explanation for the experimentally observed Lorentzian lineshapes in the rovibrational spectrum of CO, namely, the construction of an inhomogeneous spectral line from a distribution of cluster sizes. The following results show that the sparse spectral lines for individual clusters are averaged over by the droplet size distribution to form an inhomogeneously broadened spectrum that is Lorentzian in shape, accounting for the experimental observations in Ref. 15. We also analyze the size dependence of the inhomogeneous spectral line width and peak position, finding that while for large enough droplets these converge to the value in bulk helium, for intermediate sizes these show oscillations as a function of the average droplet size.

III. APPLICATION TO CO

In Fig. 2, we show the spectrum $S_{R(N)}(\omega)$ [Eq. (4b)] for the $R(0)$ transition ($J \to 1$) as a function of droplet size N and energy $E = \hbar\omega$, where we assumed a uniform droplet density $\rho = 0.02186$ Å^{-3}, such that $N = \rho(4\pi/3)R^3$. The spectral peaks occur at energies $E_i = \hbar\omega_i$, obtained from solution of Eq. (5), with weights a_i given by Eq. (6). Since for any finite R, $S_{R(N)}(\omega)$ is a stick spectrum, we have introduced a small broadening in order to show the spectral weights in Fig. 2. The spectra show clear resonances. These occur at radii R, i.e., droplet sizes N, for which $\Sigma_R(\omega)$ diverges. Recalling our discussion of the decay of the $J=1$ excitation by creation of a phonon in bulk ^{4}He in the first paragraph following Eq. (1), a necessary condition for having such a resonanance is $\ell = 0$ and $\ell' = 1$ in the finite droplet self-energy [Eq. (3)]. Thus resonances occur at N values for which the sum of the phonon energy $\epsilon(p_{\ell'=1}^{(i)})$ and the recoil energy $\hbar^2(p_{\ell'=1}^{(i)})^2/2M_0$ is close to the energy $\hbar\omega$.

As mentioned above, the peak energies E_i become denser with increasing N (see inset of Fig. 2), until a sufficiently dense set of E_i with nonvanishing weights a_i would lie in the rotation-phonon resonance region, such that, assuming finite spectral resolution, the resulting transition can be considered homogeneously broadened. Clearly, achieving this bulk limit of homogeneous broadening would require droplet sizes much larger than those generated in typical helium spectroscopy setups. In fact, if we require that the Lorentzian envelope of line width Δ contains, e.g., at least ten lines, our model yields a rough estimate of R
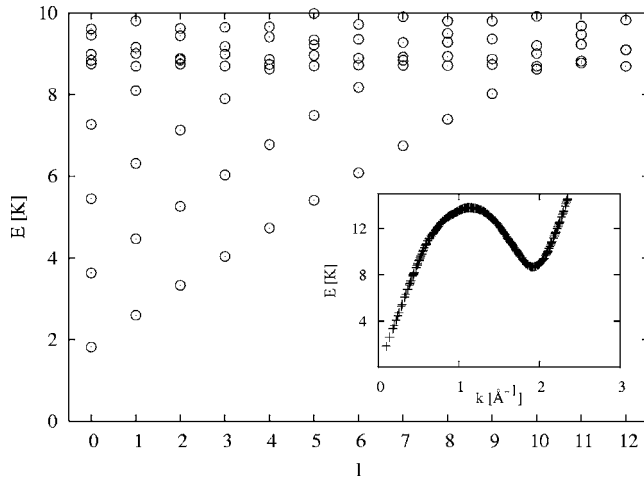
FIG. 1. The discrete phonon spectrum $\epsilon(p_\ell^{(i)})$ obtained from the boundary condition $j_\ell(p_\ell^{(i)}r)=0$ for $r=R$ (see text) is shown as function of ℓ, for $R=31.9$ Å ($N=3000$). The inset shows the same spectrum as function of the discrete momenta $p_\ell^{(i)}$, i.e., the finite size analog of the bulk dispersion relation.

$\gtrsim 10\pi\hbar c/\Delta \approx 2\times 10^4$ Å, where c is the phonon speed of sound. This corresponds to droplets larger than $N\gtrsim 10^{12}$.

The droplets formed by expansion through a nozzle have a wide range of sizes. We employ the log-normal distribution established in Ref. 27,

$$P(N) = (Nd\sqrt{2\pi})^{-1} \exp\left(-\frac{(\ln N - \mu)^2}{2d^2}\right),$$

which has an average cluster size $\bar{N}=\exp(\mu+d^2/2)$. The parameter d determines the width of the distribution and is typically less than unity. The average size $\bar{N}$ is then determined by μ, which is the second independent parameter for the size distribution.

We now have all the ingredients necessary to construct an inhomogeneous spectrum as the statistical average
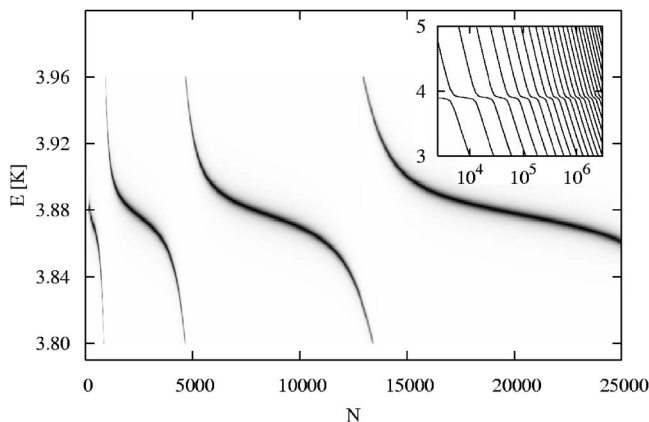

FIG. 2. The homogeneous spectrum $S_{R(N)}(\omega)$ for CO in a helium droplet is shown as a function of droplet size N and energy $E=\hbar\omega$. $R(N)$ is the radius of the cluster for a given N. For each N, $S_{R(N)}(\omega)$ is a stick spectrum. $S_{R(N)}(\omega)$ was therefore broadened by a small imaginary part $\epsilon=0.003$ K in the denominator of Eq. (4a), to allow representation of the weight. The intensity of the lines represents the magnitude of $S_{R(N)}$. The inset shows an expanded view of the peak positions up to larger N.
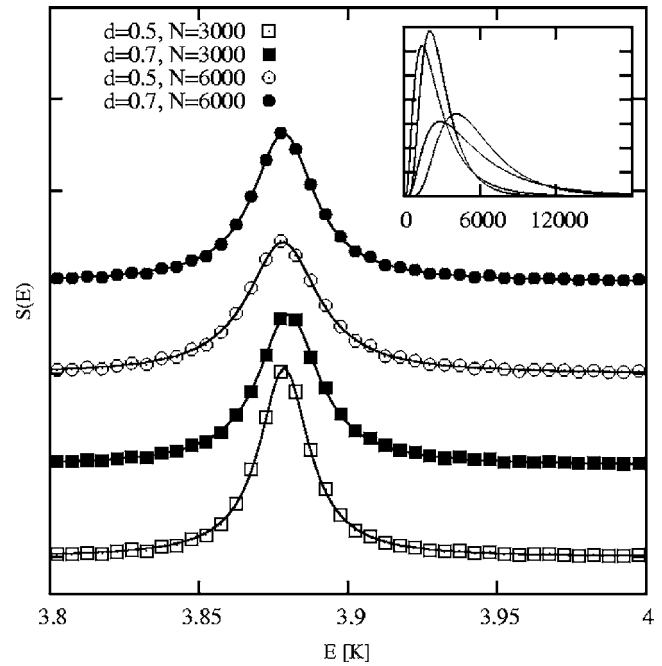

FIG. 3. The inhomogeneous rotational spectrum $S(\omega)$ of CO in ^{4}He droplets is shown for four different droplet size distributions: width parameters $d=0.5$ with average sizes $\bar{N}=3000$ and 6000 and width parameter $d=0.7$ with average sizes $\bar{N}=3000$ and 6000. The size distributions are shown in the inset. The full lines are Lorentzian fits to the spectra.

$$S(\omega) = \sum_N P(N)S_{R(N)}(\omega).$$

In Fig. 3 we show the resulting inhomogeneous spectrum for four different cluster size distributions $P(N)$ shown in the inset. Two of these distributions have a width parameter $d=0.5$ and average sizes $\bar{N}=3000$ and 6000, while the other two have a larger width parameter $d=0.7$, with the same average sizes $\bar{N}=3000$ and 6000. For all four distributions, the corresponding inhomogeneous spectrum is found to be very well fit by a Lorentzian curve. We emphasize that in all cases shown here the size distribution $P(N)$ spans only one or two resonances. This is evident from inspection of Fig. 2 over the relevant size range for the inset of Fig. 3, i.e., $0<N\leq 10^4$. Table I summarizes the line width of the spectrum $S(\omega)$ obtained from these Lorentzian fits to the droplet spectra of Fig. 3 and compares these values with the line width predicted by the CBF bulk calculation of Ref. 15. For these average sizes $\bar{N}=3000$ and 6000 the droplet values are very

TABLE I. Calculated line width (HWHM) of the inhomogeneous Lorentzian spectra for the four different cluster size distributions shown in Fig. 3. The homogeneous line width from a bulk CBF calculation is shown in the last line.

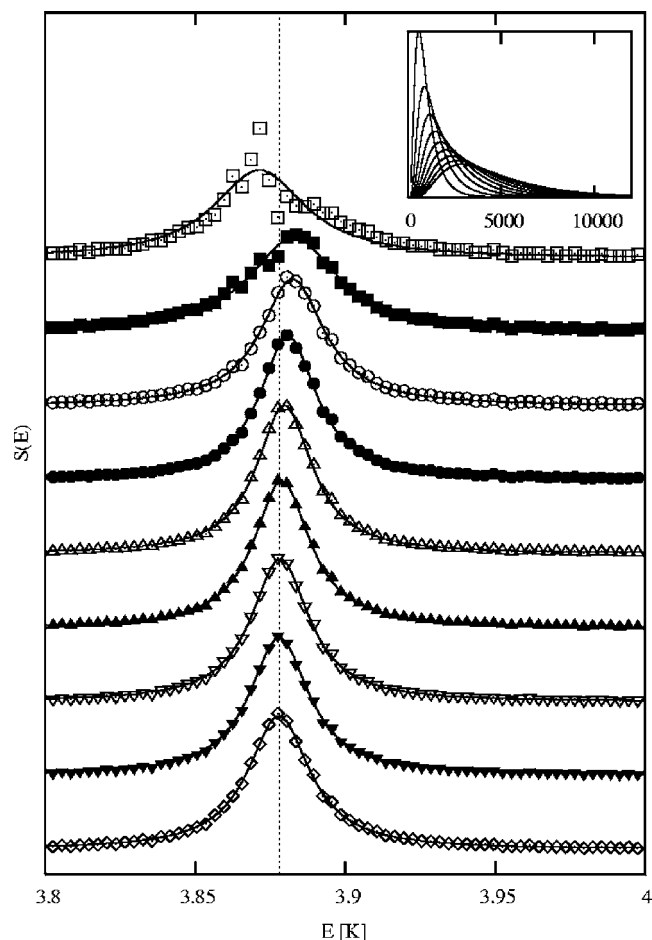| d	$\bar{N}$	$\Delta/2$ (K)
0.5	3000	0.010
0.7	3000	0.012
0.5	6000	0.014
0.7	6000	0.013
$\cdots$	∞	0.013

FIG. 4. The inhomogeneous rotational spectra $S(\omega)$ of CO in ^{4}He droplets are shown, from top to bottom, for average droplet sizes $\bar{N}$ $=1000,1500,2000,\dots,5000$ (symbols), with width parameter $d=0.6$ The corresponding droplet size distributions are shown in the inset. The full lines are Lorentzian fits to the spectra.

FIG. 5. (Color online) The rovibrational spectra measured for CO in ^{4}He droplets (Ref. 15) of average sizes ranging from $\bar{N}=1200$ to $\bar{N}=3600$. Data from Ref. 15. The red lines show Lorentzian fits to the data. The dotted line marks the center of the $\bar{N}=3600$ spectrum.

similar to each other, showing only a weak dependence on the size distribution $P(N)$. Furthermore, we note that the droplet line width values for these sizes $\bar{N}$ are close to the corresponding value from the CBF bulk calculation (bottom line of Table I).

Figure 4 shows the inhomogeneous spectrum for a range of cluster size distributions $P(N)$ with average size $\bar{N}$ varying from 1000 to 5000 in steps of 500, where the width parameter d is now kept fixed at an intermediate value $d=0.6$. The corresponding size distributions are shown in the inset. For all $\bar{N} \geq 2000$, the inhomogeneous spectra are again found to be very well fit by Lorentzian curves. For $\bar{N}=1500$ there is a very small deviation from the Lorentzian curve near the maximum and for the smaller size ($\bar{N}=1000$) the calculated spectrum deviates significantly from the Lorentzian shape, appearing to become sharper. This might be due to the fact that the width of the distribution (see insert) is becoming too narrow to adequately span the phonon resonance (Fig. 1). It might also be an indication of the limitations of the finite droplet CBF model when applied to smaller droplets where the phonons may differ from the discrete bulklike modes assumed here and the static structure factor differs increasingly from its bulk value.
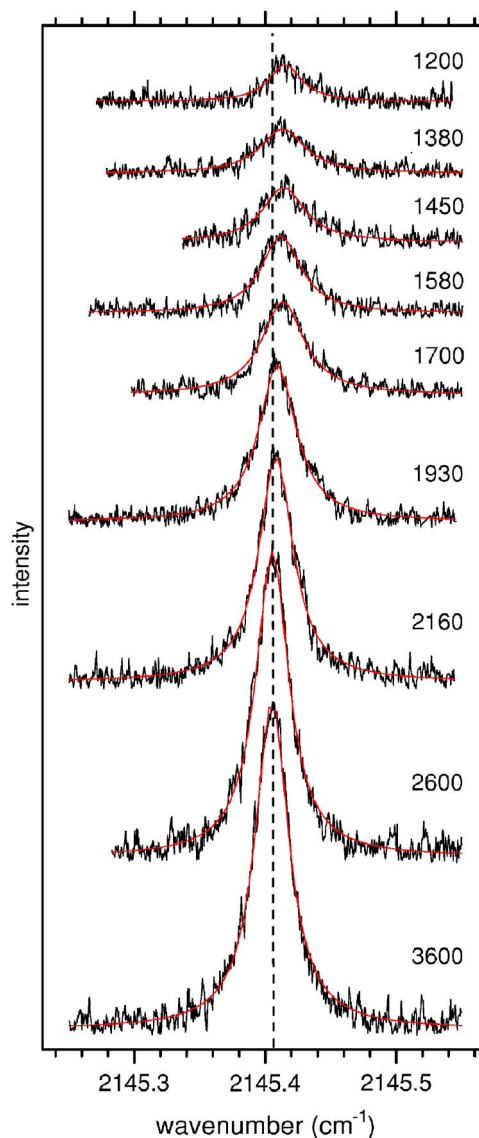
We now analyze the calculated spectral lines in Fig. 4 in more detail. The dotted line vertical line is a marker drawn through the peak location for $\bar{N}=5000$. A comparison of the peak positions for the smaller average droplet size distributions shows a small blueshift of the peak for decreasing $\bar{N}$. This is consistent with the experimental observations of Ref. 15 for $\bar{N}=1200-3600$, which are reproduced in Fig. 5. The red lines here show Lorentzian fits to the experimental rovibrational spectral line $R(0)\nu_{CO}=1\leftarrow 0$ and the dotted line provides a marker for the peak location of $\bar{N}=3600$. For comparison of the rotational contribution to the experimental shift in peak positions with our theoretical predictions from the finite droplet model, we have removed the band origin and its vibrational shift. We assumed the latter to be size independent in this droplet size range,[14] its value being determined by the isotopomer analysis presented in Ref. 15 for $\bar{N}=2600$. The resulting comparison between theory and ex-
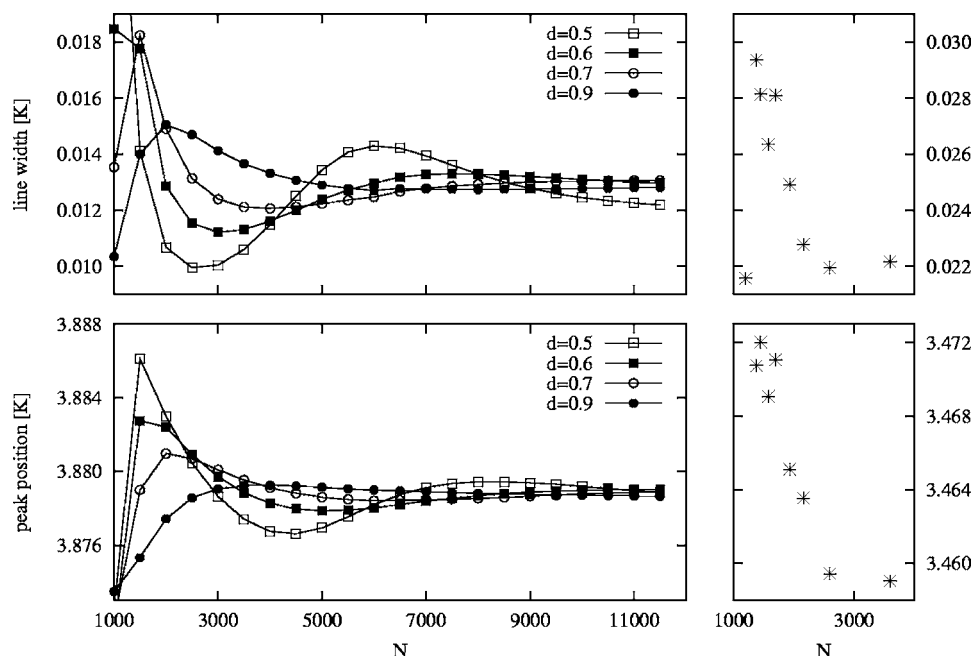
FIG. 6. The line width (HWHM, top left panel) and peak position (bottom left panel) of the rotational spectrum $S(\omega)$ of CO in ⁴He droplets are shown as a function of average droplet size $\bar{N}$. We compare here results obtained with size distributions $P(N)$ characterized by four different parameters $d=0.5$, 0.6, 0.7, and 0.9 (full lines are guides to the eye). The upper right panel shows the line width obtained from the Lorentzian fits to the experimental rovibrational spectra shown in Fig. 5. The lower right panel shows the rotational contribution to the corresponding experimental spectral peak positions, i.e., with the vibrational band origin and its shift subtracted as described in the text (also, see footnote of Ref. 42).

periment is made in Fig. 6. Here the left panels show the theoretically calculated line width and peak position of the $R(0)$ line as function of average droplet size $\bar{N}$, obtained from the Lorentzian fits shown in Fig. 4 for $d=0.6$, as well as for three other values of $d=0.5$, $d=0.7$, and $d=0.9$. For all droplet distributions $P(N)$, we see that both the calculated line width and the peak position eventually converge to the bulk value as the average size $\bar{N}$ increases. However, for smaller sizes both the line width and peak position show marked variations, which become oscillatory for small enough values of the width parameter d. These oscillations result from the size distribution $P(N)$ moving across the resonances as $\bar{N}$ increases (see Fig. 2). For example, when $P(N)$ is located below the first resonance at $N \sim 1000$, the average peak position lies below $E=3.88$ K and then as $P(N)$ moves across this resonance the spectral absorption gains a significant component of absorption at the higher energies on the upper side of the resonance so that the average peak position goes up. As $P(N)$ continues to move to larger $\bar{N}$, averaging then occurs over the flat region of Fig. 2, followed by the downward branch of the next resonance, resulting in a subsequent downward oscillation of the average peak position. The oscillations in the line width can be rationalized similarly in terms of alternating contributions from the flat and near resonant absorption regions in Fig. 2. Overall, if $P(N)$ is very broad (d is large), $P(N)$ has significant overlap with more than one resonance and the oscillatory dependence of line width and peak position with $\bar{N}$ is less pronounced. The right hand panels in Fig. 6 show the experimental line width and the rotational contribution to the peak position extracted from the fits in Fig. 5 as described above.[42] A comparison of the theoretically calculated and experimentally extracted line widths and peak positions shows good qualitative agreement in the size dependence of the line widths and peak positions, although the numerical values of these quantities differ, with the theoretical line

widths being smaller than the experimental values and the theoretical peak positions lying at systematically somewhat higher energies. Nevertheless, the theoretically calculated size dependence can be used to extract information about the size distribution, as we illustrate with the following two examples.

For width parameter $d=0.5$, the calculated line width varies by about a factor of 2 over the range $\bar{N}=1200-3600$ for $d=0.5$. In contrast, the experimental line width varies by only a factor of 0.5 up to sizes $\bar{N}=3600$. A comparison with the left panel of Fig. 6 implies then that the experimental droplet distribution must be wider than $d=0.5$. The availability of measurements over a larger size range would allow a more precise determination of the width parameter d. A second example is provided by the spectral peak position. The theoretical results in the left panel show that for $d=0.9$ the rotational shift contribution to the shift increases monotonically with $\bar{N}$, while the narrower distributions with smaller d show an initial increase followed by a decrease and subsequent oscillations at larger $\bar{N}$. The experimental values of the rotational contribution in the right panel show an initial increase followed by a decrease, consistent with a smaller value of d and excluding a width value as large as $d=0.9$.

These variations of the line width and position with the distribution parameters d and $\bar{N}$ evident in Fig. 6 above show that the distribution $P(N)$ could in principle be inferred from a precise measurement of line width and/or peak position and the dependence of these on $\bar{N}$. Clearly this would be facilitated by more experimental data at larger sizes, allowing the predicted oscillatory behavior of the line width and peak position to be explored.

The experimental setup in Ref. 15 was not able to assess whether the Lorentz-shaped spectral line is homogeneous or inhomogeneous. An unambiguous experimental answer to this question might be found with a double resonance hole-burning experiment, e.g., as in Refs. 11, 33, and 34. A

double-resonance experiment needs two independent, strong light sources. One of the light sources is fixed in frequency, and the other is scanned. The fixed light source depletes the ground state of those droplets which are in resonance with it. The other light source is scanned over the entire range of transition frequencies and probes the whole ensemble. When both frequencies match each other the probe signal will decrease according to the depletion of the ground state population, i.e., the scanning source burns a hole in the probe signal. Such a scheme will retrieve the natural line width as a dip (or "hole") in the line profile of the probe signal, provided that the bandwidth of the light sources is small enough. A double resonance experiment will therefore demand highly stabilized laser light sources. Because of the limited availability of ultrastable high resolution lasers for the rovibrational excitation of CO, other molecules may be more useful for further experimental investigation of the rotational lineshape.

IV. DISCUSSION

It is important to understand how this result of an inhomogeneous absorption with Lorentzian lineshape relates to the line width calculation that was based on the bulk CBF theory in Ref. 15. Such a bulk theory necessarily results in a homogeneous line and the conclusion there was that the $R(0)$ line is *homogeneously* broadened by the relaxation of the rotational $J=1$ excitation of the molecule coupling to a bulk phonon from the continuum of available phonon states and molecule translation states. In the present work we have found that in a finite droplet the $R(0)$ line consists of a very sparse set of one or two sharp lines that result in an *inhomogeneously* broadened spectral line due to the wide droplet size distribution characteristic of experimental droplet sources. Remarkably, these two superficially contradictory results not only agree quantitatively (for large enough droplets where the line width saturates at the bulk value, see Table I and Fig. 6), but closer analysis shows that they effectively describe very similar physical processes. Thus, in the bulk situation the line width derives from relaxation in the presence of a continuum of phonon states. In a finite droplet, the phonons are discrete and the rotational excitation can only be in resonance with a phonon if the system size is such that the molecule and phonon energies are matched [see Eq. (5)]. Since for a very short time propagation, a resonance cannot be distinguished from a decay (relaxation), the two processes are indistinguishable on a short time scale. Subsequent averaging over the system size weighted by the droplet size distribution $P(N)$ effectively averages over one full resonance, resulting in an inhomogeneous spectrum. We find that this is very similar to and, for a sufficiently broad $P(N)$, experimentally indistinguishable from the spectrum in a bulk system. This is the main result of this work. As mentioned already in the Introduction, such behavior is also found to result from an extension of the Bixon-Jorter model of coupling of a bright state to a discrete bath of harmonic dark states[32] that uses the additional assumption that the bath states are subject to a size-dependent energy shift.[30] For this model, it could be shown analytically that indeed such a

system-size induced broadening results in inhomogeneous Lorentzian lines, and that the line width is the same as in the bulk limit. Hence, our present results from the finite droplet modified CBF theory are consistent with this model of Ref. 30. In addition, the microscopic nature of the CBF theory allows us to compare with experimental results for finite size droplets. Our analysis of measured spectra for CO in ^{4}He droplets of sizes $\bar{N}=1200-3600$ shows that the CBF finite droplet theory gives good qualitative agreement with the observed size dependence of the width and spectral peak position.

Since the correlated basis function theory is generally applicable to weakly or strongly correlated quantum systems, and, in particular, to impurities in such systems,[35–39] we expect that this result may be more general, and applicable to other finite systems, e.g., to quantum dots with a large size dispersion. The general result is that the inhomogeneous spectrum of a single particle excitation coupled to discrete collective excitations of a small system is Lorentzian, provided that there is a sufficient statistical spread of system sizes to cover a full resonance. Furthermore, for large enough droplets, the spectrum is the same as the homogeneous spectrum of this single particle excitation in the bulk limit. This situation occurs even when the average size is still very far away from the bulk limit where the phonons are dense compared to the line width and the spectrum is truly homogeneous.

For smaller droplet sizes interesting oscillations in the spectral line width and peak position are found, which can be used to characterize the cluster size distributions. Oscillations with cluster sizes were observed recently for OCS and N_2O,[40,41] but the mechanism is probably a different one: The size range was two orders of magnitude smaller ($N \leqslant 80$), and the observation were made when an exact N-assignment of transitions in the spectra was accomplished, while in our work we consider inhomogeneous spectra arising from the experimental droplet size distribution.

ACKNOWLEDGMENTS

[1] C. Callegari, K. K. Lehmann, R. Schmied, and G. Scoles, J. Chem. Phys. **115**, 10090 (2001).
[2] F. Paesani, A. Viel, F. A. Gianturco, and K. B. Whaley, Phys. Rev. Lett. **90**, 073401 (2003).
[3] S. Moroni, A. Sarsa, S. Fantoni, K. E. Schmidt, and S. Baroni, Phys. Rev. Lett. **90**, 143401 (2003).
[4] N. Blinov, X. Song, and P. Roy, J. Chem. Phys. **120**, 5916 (2004).
[5] R. E. Zillich, F. Paesani, Y. Kwon, and K. B. Whaley, J. Chem. Phys. **123**, 114301 (2005).
[6] Y. Kwon and K. B. Whaley, Phys. Rev. Lett. **83**, 4108 (1999).
[7] Y. Kwon, P. Huang, M. V. Patel, D. Blume, and K. B. Whaley, J. Chem. Phys. **113**, 6469 (2000).
[8] C. Callegari, A. Conjusteau, I. Reinhard, K. K. Lehmann, G. Scoles, and F. Dalfovo, Phys. Rev. Lett. **83**, 5058 (1999). See also C. Callegari, A. Conjusteau, I. Reinhard, K. K. Lehmann, G. Scoles, and F. Dalfovo, *ibid.* **84**, 1848(E) (2000).
[9] V. S. Babichenko and Yu. Kagan, Phys. Rev. Lett. **83**, 3458 (1999).

[10] R. Zillich, Y. Kwon, and K. B. Whaley, Phys. Rev. Lett. **93**, 250401 (2004).

[11] S. Grebenev, M. Havenith, F. Madeja, J. P. Toennies, and A. F. Vilesov, J. Chem. Phys. **113**, 9060 (2000).

[12] K. Nauta and R. E. Miller, Phys. Rev. Lett. **82**, 4480 (1999).

[13] A. Conjusteau, C. Callegari, I. Reinhard, K. K. Lehmann, and G. Scoles, J. Chem. Phys. **113**, 4840 (2000).

[14] M. Hartmann, N. Pörtner, B. Sartakov, J. P. Toennies, and A. F. Vilesov, J. Chem. Phys. **110**, 5109 (1999).

[15] K. von Haeften, S. Rudolph, I. Simanovski, M. Havenith, R. Zillich, and K. B. Whaley, Phys. Rev. B **73**, 054502 (2006).

[16] K. Nauta and R. E. Miller, J. Chem. Phys. **113**, 9466 (2000).

[17] K. von Haeften, S. Rudolph, A. Metzelthin, I. Simanovski, A. Ruediger, C. Krause, and M. Havenith, Phys. Rev. Lett. **95**, 215301 (2005).

[18] K. Nauta and R. E. Miller, J. Chem. Phys. **113**, 10158 (2000).

[19] K. Nauta and R. E. Miller, J. Chem. Phys. **115**, 8384 (2001).

[20] A. M. Stoneham, Rev. Mod. Phys. **41**, 82 (1969).

[21] D. L. Orth, R. J. Mashl, and J. L. Skinner, J. Phys.: Condens. Matter **5**, 2533 (1993).

[22] A. Abragam, *Principles of Nuclear Magnetism*, International Series of Monographs on Physics (Oxford University Press, New York, 1983).

[23] C. Callegari, K. K. Lehmann, R. Schmied, and G. Scoles, J. Chem. Phys. **115**, 10090 (2001).

[24] R. Zillich and K. B. Whaley, Phys. Rev. B **6**, 104517 (2004).

[25] K. K. Lehmann, Mol. Phys. **97**, 645 (1999).

[26] S. Grebenev, M. Hartmann, M. Havenith, B. Sartakov, J. P. Toennies, and A. F. Vilesov, J. Chem. Phys. **112**, 4485 (2000).

[27] B. Dick and A. Slenczka, J. Chem. Phys. **115**, 10206 (2001).

[28] A. R. W. McKellar, J. Chem. Phys. **125**, 164328 (2006).

[29] T. Skrbic, S. Moroni, and S. Baroni, J. Phys. Chem. A **111**, 7640 (2007).

[30] K. K. Lehmann, J. Chem. Phys. **126**, 024108 (2007).

[31] D. R. Tilley and J. Tilley, *Superfluidity and Superconductivity* (Hilger, Bristol, UK, 1986).

[32] M. Bixon and J. Jortner, J. Chem. Phys. **48**, 715 (1968).

[33] I. Reinhard, C. Callegari, A. Conjusteau, K. K. Lehmann, and G. Scoles, Phys. Rev. Lett. **82**, 5036 (1999).

[34] J. M. Merritt, G. E. Douberly, and R. E. Miller, J. Chem. Phys. **121**, 1309 (2004).

[35] E. Krotscheck, M. Saarela, and J. Epstein, Phys. Rev. B **38**, 111 (1988).

[36] B. E. Clements, E. Krotscheck, and M. Saarela, Phys. Rev. B **55**, 5959 (1997).

[37] E. Krotscheck and R. Zillich, Phys. Rev. B **58**, 5707 (1998).

[38] E. Krotscheck and R. Zillich, J. Chem. Phys. **115**, 10161 (2001).

[39] E. Krotscheck, M. Saarela, K. Schörkhuber, and R. Zillich, Phys. Rev. Lett. **80**, 4709 (1998).

[40] A. R. W. McKellar, Yunjie Xu, and W. Jäger, Phys. Rev. Lett. **97**, 183401 (2006).

[41] A. R. W. McKellar, J. Chem. Phys. **127**, 044315 (2007).

[42] The width for the $\bar{N} = 2600$ spectrum shown here is 0.022 K, somewhat less than the value of 0.024 K reported in Ref. 15 that was derived by averaging over many tens of such individual spectra.